Hydrogen Bond Dynamics Probed with Ultrafast Infrared Heterodyne-Detected Multidimensional Vibrational Stimulated Echoes

John B. Asbury, Tobias Steinel, C. Stromberg, K. J. Gaffney, I. R. Piletic, Alexi Goun, and M. D. Fayer
Department of Chemistry, Stanford University, Stanford, California 94305, USA
(Received 24 February 2003; published 3 December 2003)

Hydrogen bond dynamics are explicated with exceptional detail using multidimensional infrared vibrational echo correlation spectroscopy with full phase information. Probing the hydroxyl stretch of methanol-OD oligomers in CCl_4, the dynamics of the evolving hydrogen bonded network are measured with ultrashort (< 50 fs) pulses. The data along with detailed model calculations demonstrate that vibrational relaxation leads to selective hydrogen bond breaking on the red side of the spectrum (strongest hydrogen bonds) and the production of singly hydrogen bonded photoproducts.

DOI: 10.1103/PhysRevLett.91.237402 PACS numbers: 78.30.Cp, 78.47.+p, 82.30.Rs, 82.50.Bc

Hydrogen bonding liquids, such as alcohols and water, have complex structures and dynamics. Such liquids have generated a great deal of experimental [1–5] and theoretical [6–9] study because of their importance as solvents in chemical and biological systems. Properties of hydrogen bond networks can be studied using infrared spectroscopy of the hydroxyl stretching mode because of the influence of the number and strength of hydrogen bonds on the hydroxyl stretch frequency [10]. A water molecule can form up to four hydrogen bonds, and the various number and types of hydrogen bonds are not spectroscopically resolvable under the broad hydrogen bonded hydroxyl stretch band [6]. In contrast, molecular dynamics simulations demonstrate that methanol predominantly forms two hydrogen bonds, whether in the pure liquid [8] or as oligomers in CCl_4 [9]. The description of the structure and evolution of hydrogen bonded networks in methanol is greatly simplified compared to water by the preponderance of a single conformation in which each methanol is a single hydrogen bond donor and a single acceptor. These are called δ, which absorb at $\sim$2490 cm^{-1} (FWHM $\sim$ 150 cm^{-1}). For oligomers that are not rings, each oligomer has two ends. One end is a hydrogen bond donor but not an acceptor called γ, which absorbs at $\sim$2600 cm^{-1} (FWHM $\sim$ 80 cm^{-1}). The other end is a hydrogen bond acceptor but not a donor called β, which absorbs at $\sim$2690 cm^{-1} (FWHM $\sim$ 20 cm^{-1}) [3]. All three of these species are spectroscopically resolvable. Consequently, methanol oligomers in CCl_4 are an important system for studying the dynamics of hydrogen bonded networks [2].

Here we report the first application of ultrafast heterodyne detected multidimensional stimulated vibrational echo correlation spectroscopy with full phase information to the study of the dynamics of hydrogen bonding liquids. The development of the ultrafast infrared vibrational echo technique [11,12] and the recent extension to multidimensional vibrational echo methods [13] provide a new approach for the study of condensed matter systems. By using the shortest mid-IR pulses produced to date ($<$50 fs or $<$4 cycles of light), it is possible to simultaneously examine the entire broad hydroxyl stretching band of methanol-OD (MeOD, deuterated hydroxyl) oligomers in CCl_4 solution despite its $>$400 cm^{-1} width. Data are obtained with correct phase relationships across the entire spectrum, which permits accurate separation of the absorptive and dispersive contributions to the spectra. As a result, the 2D IR correlation spectra are akin to 2D NMR spectra [14]. The experimental results and model calculations demonstrate the selective breaking of the strongest hydrogen bonds through a nonequilibrium relaxation pathway that precedes vibrational energy equilibration.

For the experiment, the $<$50 fs transform limited IR pulses are generated using a Ti:sapphire regeneratively amplified laser/optical parametric amplifier system. The IR beam is split into five beams. Three of the beams are the excitation beams for the stimulated vibrational echo. A fourth beam is the local oscillator (LO) used to heterodyne detect the vibrational echo signal. The vibrational echo signal combined with the LO is passed through a monochromator and detected by a 32 element mercury cadmium telluride array. The monochromator is stepped to cover the entire spectrum. The sample, 10% MeOD in CCl_4, was held in a sample cell of CaF_2 flats with a spacing of 50 μm. A fifth beam is the probe in pump-probe experiments.

The multidimensional stimulated vibrational echoes were measured as a function of one frequency variable, ω_m (monochromator/array), and two time variables, τ (time between pulses 1 and 2) and T_w (time of third pulse after the first two pulses). The measured signal is the absolute value squared of the sum of the vibrational echo signal electric field, S, and the local oscillator electric field, L. The spectrum of the cross term, $2LS$, is the ω_m frequency axis. Scanning τ generates an interferogram. Numerical Fourier transformation converts the interferogram into the frequency variable ω_τ, which contains both the absorptive and dispersive components of the signal. However, two sets of quantum pathways

can be measured independently by appropriate time ordering of the pulses [13]. By adding the Fourier transforms of the interferograms from the two pathways, the dispersive component cancels, leaving only the absorptive component.

Lack of perfect knowledge of the timing of the pulses and consideration of chirp on the vibrational echo pulse requires a "phasing" procedure to be used. The projection slice theorem [14] is employed to generate the absorptive 2D correlation spectrum that is compared to the experimental pump-probe spectrum. The procedure requires a comprehensive mathematical formulation and implementation that will be detailed subsequently.

Figure 1 displays some of the 2D correlation spectra, four contour plots at $T_w = 125$, 1.2, 1.8, and 5.0 ps for MeOD. The maximum positive signal has been normalized to unity in each plot. The contours represent equal 10% graduations. The ω_τ axis is the axis of the first radiation field interaction. The ω_m axis is the axis of the emission of the echo pulse. The positive going band on the diagonal in the 125 fs spectrum corresponds to the 0–1 transition of the δ band with some contribution from the 0–1 γ band on the blue end. The center frequencies of the δ and γ 0–1 transitions are indicated by horizontal and vertical lines. The negative going band below the main diagonal band arises from the 1–2 transition of the δ band. The 1–2 band is off diagonal because the emission is shifted to lower frequency by the vibrational anharmonicity ($\sim$150 cm^{-1}).

As the T_w delay increases, the correlation spectra displayed in Fig. 1 exhibit changes that provide insight into the mechanism of hydrogen bond evolution. By $T_w =$ 1.2 ps, the correlation spectrum has changed dramatically due to vibrational relaxation and hydrogen bond breaking. A good fraction of the initially produced excited state population has decayed to the ground state because the vibrational lifetime of the δ OD stretch is $\sim$0.5 ps [2]. By $T_w = 1.8$ ps, the δ excited state has completely decayed. Because the lifetime of the γ band ($\sim$1 ps) is longer than that of the δ band, the diagonal γ 0–1 band is uncovered as the δ band decays. By $T_w =$ 1.8 ps, the diagonal γ peak is almost gone.

As will be demonstrated below, when the δ OD excited state relaxes, hydrogen bonds break [1,2], producing photoproduct γ ODs. The resulting photoproduct γ peak, located above the δ band, is visible by $T_w =$ 1.2 ps. By $T_w = 5.0$ ps, the only remaining features are the preserved δ and the photoproduct γ bands. Comparison of the center of the preserved δ band at $T_w =$ 5.0 ps and the center of the initially excited δ band (indicated by the horizontal line at 2490 cm^{-1}) demonstrates that the preserved δ band is contracted to the red and shifted off diagonal along the ω_m axis. For times longer than $\sim$5 ps, the peaks do not change shape significantly, but slowly decay in magnitude on a time scale of tens of ps because of hydrogen bond recombination [1,2]. An important aspect of the 2D correlation spectrum is that the photoproduct γ is spectrally separated in the plane from the equilibrium γ band (see Fig. 1, $T_w =$ 1.2 and 1.8 ps), in contrast to 1D spectroscopies.

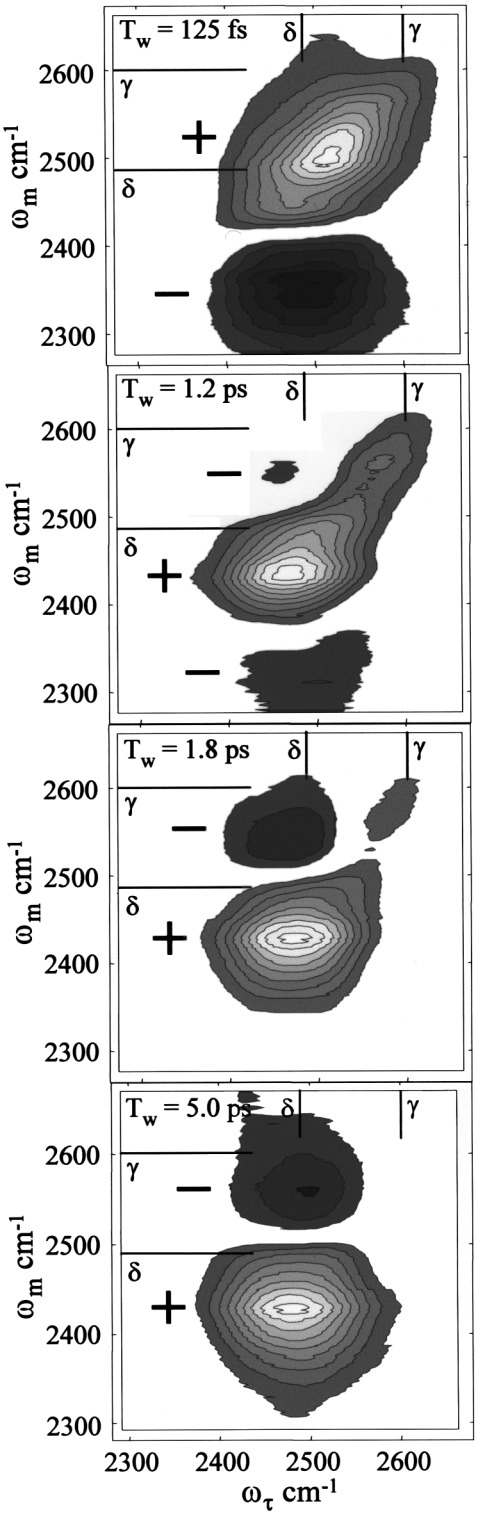

FIG. 1. Correlation spectra for several T_w delays. See text for details.

The T_w dependence of the correlation spectra raises a number of questions. First, why does a correlation spectrum exist for times long compared to the vibrational lifetime? Normally, the decay of the excited state into the ground state causes the vibrational echo signal to decay. However, following vibrational relaxation, a few tens of percent of the initially excited δs break a hydrogen bond in ~200 fs, removing them as δ absorbers and creating new photoproduct γ absorbers [2]. Therefore, the decay of the excited state does not completely eliminate the contribution to the signal from the ground state. The ground state signal remains for the hydrogen bond recombination time, which is tens of ps [1,2].

Second, a fundamentally important question that will be addressed here is whether vibrational relaxation simply "heats" the hydrogen bond network following vibrational relaxation or is there another mechanism that gives rise to the time dependence of the bands shown in Fig. 1? To address this question, we have performed detailed calculations to model the correlation spectra. The four models will be described in detail in a future publication. For brevity, we give a very brief overview of the modeling procedure and discuss only the two models that gave the best results. The correlation spectra are fit using the sum of 2D Gaussian band shapes for the δ and γ, 0–1 and 1–2 bands. For the $T_w = 125$ fs correlation spectrum, the widths and positions of the bands are set equal to the equilibrium δ and γ widths and positions as determined from linear spectroscopy of the sample. The $T_w = 125$ fs correlation spectrum is very well described by this model. The calculations use results of the fits to the 125 fs data and factors that are unique to each model to calculate the 5 ps data. The 1–2 bands do not contribute because 5 ps is much longer than the lifetime.

The experiments also give the ratios of the amplitudes of the 0–1 bands at 125 fs to those at 5 ps. From comparison of the fit to the $T_w = 125$ fs correlation spectrum with the fit to the 5 ps correlation spectrum using each model, the ratios of the amplitudes are determined for each model.

Model 1.—Following vibrational relaxation of the initially excited OD stretch, the deposited energy (heat) causes hydrogen bond weakening. Weakening of hydrogen bonds shifts their absorption to the blue (higher energy) [10]. The δ and γ bleach responsible for the long lived vibrational echo signal is not filled in by the vibrational relaxation because the population is shifted to the blue. The center positions and widths of the preserved δ and γ bleach bands are described by their equilibrium spectra. The weakened δ and γ photoproducts have spectra that are shifted to the blue along the ω_m axis. In the calculations, the magnitude of the blueshift is allowed to vary to give the best fit to the 5 ps data ($R^2 = 1.1$, residuals squared). The correlation spectrum calculated from model 1 is displayed in Fig. 2(a). The model does a reasonable job of reproducing aspects of the data (compare to lowest panel of Fig. 1). However, it does not have the correct shape. The preserved band (positive going) is elongated to the upper right because of the preserved γ portion of the spectrum. Even more significant, to obtain this best fit, the amplitudes of the bands are unphysical. To get the features in the correct positions along the ω_m axis requires a very small shift (5 cm^{-1}) of the weakened band produced by vibrational relaxation. Because of the small shift, the preserved δ bleach band strongly overlaps and nearly cancels the weakened photoproduct band. To obtain the correct ratio of the amplitude of the $T_w = 5.0$ ps data relative to the 125 fs data, model 1 requires the magnitude of the preserved δ bleach band to be ~9 times larger than the magnitude of the initial δ bleach, which would require the concentration of initially excited MeODs *increasing* by a factor of ~9 between $T_w = 125$ fs and 5.0 ps. Obviously this result is not possible. Model 1 cannot describe the data. Model 1 is essentially a thermal equilibration model. Detailed measurements of the pump-probe spectrum show that it takes ≥ 30 ps for the system to reach thermal equilibrium (after which the pump-probe spectrum is the same as the static temperature difference spectrum). The time dependent pump-probe spectrum again demonstrates that the mechanism that gives rise to the 5 ps data is not thermal equilibration.

Model 2.—Vibrational relaxation of initially excited OD stretches selectively breaks hydrogen bonds on the red side of the δ band and produces redshifted γ photoproducts. In the calculations, the spectral region of hydrogen bond breaking is allowed to vary to give the best fit to the 5 ps data ($R^2 = 0.13$). The simulated correlation spectrum calculated from model 2 is displayed in Fig. 2(b). This model provides an excellent description of the $T_w = 5.0$ ps experimental data. The shape of the spectrum is correct, and the R^2 value is a factor of ~8 smaller for model 2 compared to model 1. In addition to having the correct shape and a better R^2, model 2 predicts a physically reasonable magnitude for the amplitudes of

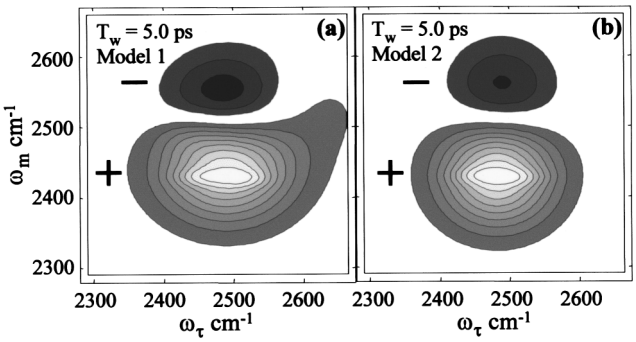

FIG. 2. Calculated correlation spectra from two models of hydrogen bond evolution following vibration relaxation. See text for details.

the bands at 5 ps relative to 125 fs. Model 2 gives the preserved δ bleach to ~60% of the initial δ bleach, that is, 60% of the initially excited δ MeODs break a hydrogen bond, which is within a few tens of percent of the value determined by independent measurements of the quantum yield of hydrogen bond breaking in MeOD oligomers [2].

The results presented above demonstrate that the δ band is contracted to the red and the photoproduct γ band is generated because vibrational relaxation selectively breaks the stronger hydrogen bonds (the red side of the line). The breaking of the strongest hydrogen bonds is at first surprising. However, this nonequilibrium mechanism can occur if vibrational relaxation on the low energy side of the line populated different modes than vibrational relaxation on the high energy side of the line, and the modes populated through the lower energy relaxation pathway are more effective at breaking hydrogen bonds. Significant support for the proposed nonequilibrium mechanism comes from the IR pump/Raman probe experiments of Iwaki and Dlott, who observed that the pathway for vibrational relaxation was different on the red and blue sides of the hydroxyl stretching band in OH methanol [15]. Excitation on the red side led to vibrational relaxation that produced substantially more relative population of hydroxyl bends compared to excitation on the blue side that put much more population in the CH bends and other modes [15]. The hydroxyl bends would be expected to be strongly coupled to the hydrogen bond in contrast to CH stretches. This necessary feature of the proposed mechanism is indeed observed experimentally.

Finally, two types of frequency correlation between the initially excited δ and photoproduct γ bands are observed. These will be discussed in detail subsequently, but, briefly, the first type, which we call coarse correlation, is observed in the redshift along the ω_m axis of the preserved δ and photoproduct γ bands at $T_w = 5.0$ ps (compare to the equilibrium δ and γ band positions marked in Fig. 1). The redshift indicates that breaking the strongest hydrogen bonds associated with δs creates photoproduct γs that retain coarse "memory" of the hydrogen bond strengths. However, detailed analysis of the time dependent 2D shape of the photoproduct γ peak demonstrates that a fine correlation also exists. Briefly, the width along the ω_τ axis of the 2D photoproduct γ peak displays the dynamical linewidth. Changes in the dynamical linewidth report the spectral diffusion dynamics. Analysis of the dynamical linewidth of the photoproduct γ peak as a function of T_w demonstrates that spectral diffusion occurs in the photoproduct γ peak on the tens of ps time scale. Observation of spectral diffusion dynamics in the photoproduct γ band proves that the broken oligomers retain a "fine" as well as a coarse memory of the structural degrees of freedom of the network prior to hydrogen bond breaking.

Here we have presented the first application of vibrational echo correlation spectroscopy to the study of hydrogen bond network dynamics. The experiments covered the entire very broad spectral region with full phase information using ultrashort midinfrared pulses. For brevity, the analysis focused on the nonequilibrium hydrogen bond breaking dynamics following vibrational relaxation that results in selective breaking of the stronger hydrogen bonds. The data also provide unique information, which will be presented subsequently, on spectral diffusion that describes hydrogen bond evolution prior to and following hydrogen bond breaking.

This work was supported by the AFOSR (F49620-01-1-0018), DOE (DE-FG03-84ER13251), and NSF (DMR-0088942). T. S. thanks the Emmy Noether program of the DFG for partial support.

[1] R. Laenen and C. Rausch, J. Chem. Phys. **106**, 8974 (1997).
[2] K. J. Gaffney *et al.*, J. Phys. Chem. A **106**, 12012 (2002).
[3] S. Woutersen, U. Emmerichs, and H. J. Bakker, J. Chem. Phys. **107**, 1483 (1997).
[4] G. M. Gale *et al.*, Phys. Rev. Lett. **82**, 1068 (1999).
[5] S. Yeremenko, M. S. Pshenichnikov, and D. A. Wiersma, Chem. Phys. Lett. **369**, 107 (2003).
[6] C. P. Lawrence and J. L. Skinner, J. Chem. Phys. **118**, 264 (2003).
[7] R. Rey, K. B. Møller, and J. T. Hynes, J. Phys. Chem. A **106**, 11993 (2002).
[8] D. M. zum Buscheenfelde and A. Staib, Chem. Phys. **236**, 253 (1998).
[9] R. Veldhuizen and S. W. de Leeuw, J. Chem. Phys. **105**, 2828 (1996).
[10] A. Novak, in *Structure and Bonding*, edited by J. D. Dunitz (Springer-Verlag, Berlin, 1974), Vol. 18, p. 177.
[11] D. Zimdars *et al.*, Phys. Rev. Lett. **70**, 2718 (1993).
[12] P. Hamm, M. Lim, and R. M. Hochstrasser, Phys. Rev. Lett. **81**, 5326 (1998).
[13] M. Khalil, N. Demirdöven, and A. Tokmakoff, J. Phys. Chem. A **107**, 5258 (2003).
[14] R. R. Ernst, G. Bodenhausen, and A. Wokaun, *Nuclear Magnetic Resonance in One and Two Dimensions* (Oxford University Press, Oxford, 1987).
[15] L. K. Iwaki and D. D. Dlott, J. Phys. Chem. A **104**, 9101 (2000).